A GLRT Approach to Data-Aided Timing Acquisition in UWB Radios—Part II: Training Sequence Design

Zhi Tian, *Member, IEEE*, and Georgios B. Giannakis, *Fellow, IEEE*

***Abstract*—The overall system efficiency of impulse radio communications relies critically on judicious allocation of transmission resources, a portion of which should be used to ensure successful timing acquisition. In data-aided mode, optimum timing offset estimation depends not only on the mechanism used for energy capture and the acquisition algorithm employed to recover timing information, but also on the training sequence (TS) pattern from which the timing information is to be extracted. Furthermore, the transmission resources used for timing have to be balanced with that for conveying information messages in order to strike desirable tradeoffs between timing accuracy and information rate. In Part I of this paper, data-aided timing offset estimation is derived based on the maximum likelihood (ML) criterion, where only symbol-rate samples are needed for low-complexity receiver processing. To minimize the mean-square timing errors of these ML synchronizers while at the same time maximizing the average system capacity, TS design and transmit power allocation are investigated in this paper. The optimum training pattern and the number, placement, and power distribution between training and information-bearing symbols are formulated as a resource allocation optimization problem whose solution optimizes system-level performance with the minimum amount of resources consumed.**

***Index Terms*—Data-aided estimation, timing acquisition, training sequence (TS) design, transmission resource allocation, ultrawide-band (UWB) communications.**

I. Introduction

ULTRAWIDE-BAND (UWB) radios have spurred great interest in both academia and industry for their potential use in high-speed short-range wireless multiple access with capability to overlay existing channelized RF services [1]–[3]. The attractive features of UWB impulse radios stem from their unique transmission structure: a stream of ultrashort (on the order of sub-nanoseconds) pulses transmitted at very low power density with a low duty cycle. To maintain adequate signal energy for reliable detection, each symbol is transmitted over a large number of frames with one pulse per frame. As a result, acquisition (a.k.a. coarse timing) is required at the frame level to find out when the first frame in each symbol starts. The acquisition task is particularly critical to reliable transmissions over dense multipath propagation environments [2], [4]–[6], where symbol detection performance is relatively robust to where each symbol starts within its first frame—a task to be accomplished by tracking (a.k.a. fine timing) schemes [7].

The unique UWB transmission format, on the other hand, imposes a great challenge to timing acquisition. Conventional sliding-correlation-based synchronization techniques require a long search time and an unreasonably high sampling rate at several gigahertz [4]. The complexity issue is further exacerbated by the performance degradation incurred by dense multipath propagation [8], [9] and by the time-hopping code used for smoothing the transmitted spectrum and for enabling multiple access. Without properly accounting for the unique features of UWB transmissions, synchronization methods that are well suited for narrowband systems are no longer effective.

Taking a data-aided maximum likelihood (ML) approach, we derived in a companion paper [10] a generalized likelihood ratio test (GLRT) for joint detection and frame-level timing acquisition, where channel-dependent unknowns are regarded as nuisance parameters. The GLRT approach yields the channel-dependent amplitude estimates, the timing acquisition solution, the symbol detection rule, as well as the associated estimation performance bounds. It was observed that the training sequence (TS) design directly affects this GLRT solution as well as the corresponding Cramer–Rao bound (CRB) of the acquisition error. In binary transmissions, the GLRT suggests that the training symbol subsets used for channel estimation and for timing acquisition should be nonoverlapping, whereas the timing accuracy is affected by both TS subsets due to its dependence on nuisance channel parameters. Therefore, judicious design of the TS pattern is desired to optimize the timing performance.

Based on the acquisition solutions and the associated performance bounds that we obtained in [10], we explore in this paper the optimum allocation of training resources to different TS subsets, where the design parameters include the placement, power, and number of training symbols. The goal is to minimize the timing estimation CRB under the constraints on total training resources. Furthermore, at a system level, those

Manuscript received February 12, 2004; revised August 15, 2004; accepted October 11, 2004. The editor coordinating the review of this paper and approving it for publication is G. M. Vitetta. The work of Z. Tian was supported by the National Science Foundation (NSF) under Grant CCR-0238174 and Grant ECS-0427430. The work of G. B. Giannakis was supported by the Army Research Laboratory/Collaborative Technology Alliance (ARL/CTA) under Grant DAAD19-01-2-011 and by the National Science Foundation-Information Technology Research (NSF-ITR) under Grant EIA-0324864. This paper was presented in part at the International Conference on Communications (ICC'2004), Paris, France, June 2004.

Z. Tian is with the Department of Electrical and Computer Engineering, Michigan Technological University, Houghton, MI 49931 USA (e-mail: ztian@mtu.edu).

G. B. Giannakis is with the Department of Electrical and Computer Engineering, University of Minnesota, Minneapolis, MN 55455 USA (e-mail: georgios@ece.umn.edu).

Digital Object Identifier 10.1109/TWC.2005.858345

resources have to be balanced with that for information-bearing symbols in order to strike desirable rate–performance tradeoffs: more training symbols improve both timing and symbol estimation but also reduce transmission rate. To this end, we also investigate the optimum power and number allocation between training symbols and information-bearing symbols. We select transmission parameters to jointly optimize timing offset estimation performance and average system capacity.

The rest of the paper is organized as follows. Section II briefly outlines the data-aided optimum ML timing acquisition solution obtained in [10], where two distinct subsets of training symbols are used to jointly carry out the symbol synchronization task. TS design in terms of judicious allocation of training resources between two different subsets is investigated in Section III, while system-level transmission resource allocation between training and information symbols is studied in Section IV. Simulations and comparisons are presented in Section V, followed by concluding remarks in Section VI.

II. Preliminaries

Consider the UWB transmission model using pulse amplitude modulation (PAM) [3]. Every information symbol $s[n] \in \{\pm 1\}$ is transmitted using N_f pulses over N_f frames, with one pulse per frame of frame duration T_f. The symbol-level waveform of duration $T_s := N_f T_f$ is $p_s(t) = \sum_{j=0}^{N_f-1} p(t - jT_f - c_j T_c)$, where $p(t)$ is a unit energy ultrashort monocycle of duration T_p at the nanosecond scale and the chip sequence $\{c_j\}$ represents a user-specific pseudorandom time-hopping (TH) code with $c_j T_c < T_f$, $\forall j \in [0, N_f - 1]$. Letting $\mathcal{E}_{t,0}$ denote the transmission energy per training symbol (including all N_f pulses), the transmitted PAM UWB waveform is

$$u(t) = \sqrt{\frac{\mathcal{E}_{t,0}}{N_f}} \sum_{n=-\infty}^{\infty} s[n] p_s(t - nN_f T_f). \tag{1}$$

The signal $u(t)$ propagates through an L-path fading channel with path gains α_l and delays τ_l satisfying $\tau_0 < \tau_1 < \cdots < \tau_{L-1}$. The timing information of interest refers to the first arrival time τ_0, which we express as $\tau_0 := n_s T_s + n_f T_f + \epsilon$. Without loss of generality, we assume that the receiver sets the initial timing at $t = 0$; thus, the timing parameter $n_s := \lfloor \tau_0 / T_s \rfloor \geq 0$ ($\lfloor \cdot \rfloor$ stands for integer floor) denotes the symbol-level offset, $n_f \in [0, N_f - 1]$ the frame-level offset, and $\epsilon \in [0, T_f)$ the pulse-level offset, respectively. Defining $\tau_{l,0} := \tau_l - \tau_0$, with $0 \leq \tau_{l,0} \leq T_f - T_p - (C_{Nf-1} - C_0)T_c$, the composite channel formed by convolving the physical channel impulse response with the transmitted pulse $p(t)$ can be expressed as $g(t) = \sum_{l=0}^{L-1} \alpha_l p(t - \tau_{l,0})$, while the time-dispersed received symbol waveform of duration T_s is $g_s(t) = \sum_{j=0}^{N_f-1} g(t - jT_f - c_j T_c) = \sum_{l=0}^{L-1} \alpha_l p_s(t - \tau_{l,0})$. The waveform at the output of the receiver antenna is then given by

$$r(t) = \sqrt{\frac{\mathcal{E}_{t,0}}{N_f}} \sum_{n=-\infty}^{\infty} s[n] g_s(t - nT_s - n_s T_s - n_f T_f - \epsilon) + w(t) \tag{2}$$

where the wide sense stationary process $w(t)$ accounts for both thermal noise and multiple access interference, which, similar to [11], is approximated as zero-mean white Gaussian with double-sided power spectrum density $\mathcal{N}_o/2$.

A symbol-by-symbol sliding correlation receiver is applied to yield samples at the symbol rate by

$$y[n] := \int_{nT_s}^{(n+1)T_s} r(t) p_{rs}(t - nT_s) dt \tag{3}$$

where $p_{rs}(t)$, $t \in [0, T_s]$, is the receiver correlation template. A simple sliding correlator uses $p_{rs}(t) = p_s(t)$, while an optimum matched filter under perfect timing corresponds to $p_{rs}(t) = g_s(t)$, which is equivalent to maximum ratio combining, but unfortunately entails an insurmountable task of estimating a large number of closely spaced delays $\{\tau_{l,0}\}$ and their amplitudes $\{\alpha_l\}$. Alternatively, transmit reference [12], [13] or pilot waveform assisted modulation (PWAM) [14] can be used to generate a noisy version of $g_s(t)$ from $r(t)$ followed by simple integrate-and-dump operations to yield $y[n]$. For any template $p_{rs}(t)$, the sample $y[n]$ can be expressed as [10]

$$y[n] = A_\epsilon \left(s[n - n_s] \left(N_f - (n_f + \lambda_{g,\epsilon}) \right) + s[n - n_s - 1](n_f + \lambda_{g,\epsilon}) \right) + w[n] \tag{4}$$

where $A_\epsilon := \sqrt{\mathcal{E}_{t,0}/N_f} \mathcal{A}_\epsilon$ (with $\mathcal{A}_\epsilon := (1/N_f) \int_0^{T_s} \sum_{q=0}^{1} g_s (t - \tau_0 + qT_s) p_{rs}(t) dt$) denotes the correlator output when there is no data modulation. The quantity $\mathcal{A}_\epsilon$ is the discrete-time symbol-rate-sampled effective channel amplitude that captures the effects of the transmit filter, the multipath propagation, and the receive template. The scalar $\lambda_{g,\epsilon}$ is a small adjustment factor to n_f that is bounded between [0, 1], which arises due to the channel delay spread, the TH code, and the unknown tracking offset [10].

Equation (4) clearly establishes the effects of different levels of timing offset on the symbol rate correlator output. Each sample $y[n]$ at the correlator output entails up to two consecutive symbols in the presence of timing offset, with the symbol indices determined by the symbol-level offset n_s. While the energy capture in the form of the effective channel amplitude A_ϵ is affected by ϵ within a frame, the amplitude scale factor of the mistiming-induced intersymbol interference (ISI) term is determined by $\nu_{f,\epsilon} := n_f + \lambda_{g,\epsilon}$, where $n_f = \lfloor \nu_{f,\epsilon} \rfloor$ since $\lambda_{g,\epsilon} \in [0, 1]$. For resource allocation among training symbols, we seek to minimize the variance of the frame-level timing offset estimator $\hat{\nu}_{f,\epsilon}$. As such, we will neglect the bounded $\lambda_{g,\epsilon}$ because its contribution to the acquisition variance is independent of that of training symbols. The effect of $\lambda_{g,\epsilon}$ will be taken into account at the system level when discussing resource allocation between training and information-bearing symbols. For this reason, we set $\lambda_{g,\epsilon} = 0$ for the time being; thus, $\nu_{f,\epsilon} = n_f$.

Given N samples $\{y[n]\}_{n=0}^{N-1}$, the goal of data-aided timing acquisition is to optimally estimate n_s and n_f based

on N_t training symbols $\{s[n]\}_{n=0}^{N_t-1}$, which arrive at the receiver during $[\tau_0, \tau_0 + N_t T_s]$. Without knowing when the UWB stream starts, a synchronizer collects $N > N_t$ observations $\mathbf{y} := [y[0], \ldots, y[N-1]]^T$ over the interval $[0, NT_s]$. Taking on a GLRT approach, we formulated in [10] a binary hypothesis testing problem for detecting the UWB signal [cf. (4)], i.e.,

$$\begin{aligned} H_1 : y[n] &= A_\epsilon \left(s[n-n_s](N_f - \nu_{f,\epsilon}) \right. \\ &\quad \left. + s[n-n_s-1]\nu_{f,\epsilon}\right) + w[n], \\ &\quad n = n_s, \ldots, n_s + N_t - 1 \leq N-1 \qquad (5) \\ H_0 : y[n] &= w[n], \qquad n = 0, 1, \ldots, N-1. \qquad (6) \end{aligned}$$

This is a classical detection problem where data under both hypotheses have the same variance but differ in their respective means. Since there are several unknown parameters in (5), namely, A_ϵ, $\nu_{f,\epsilon}$, and n_s, the GLRT is well motivated. Accordingly, we reject H_0 if the log-likelihood ratio (LLR) satisfies

$$\begin{aligned} J(\mathbf{y}; A_\epsilon, n_s, \nu_{f,\epsilon}) &:= 2\sigma_w^2 \log_2 \frac{p(\mathbf{y}; \hat{A}_\epsilon, \hat{n}_s, \hat{\nu}_{f,\epsilon}, H_1)}{p(\mathbf{y}; H_0)} \\ &\leq 2\sigma_w^2 \log_2 \mathcal{T}_{\mathrm{FA}} \qquad (7) \end{aligned}$$

where $\hat{A}_\epsilon$, $\hat{n}_s$, and $\hat{\nu}_{f,\epsilon}$ are the corresponding ML estimates (MLEs) under H_1, and $\mathcal{T}_{\mathrm{FA}}$ is a threshold set by the desired probability of false alarms (FA). The noise term $w[n]$ is assumed to be Gaussian distributed with known (or measured) variance σ_w^2. When seeking the (conditional) MLEs of the unknown nuisance parameters, we assume that A_ϵ, $\nu_{f,\epsilon}$, and n_s are deterministic.

For binary PAM, the correlator output samples under H_1 can be split in two groups: one group, denoted by $\mathbf{y}_+[n_s] := \{y[n] : n \in \mathcal{G}_+(n; n_s)\}$, is indexed by all the n's in the set $\mathcal{G}_+(n; n_s) := \{n : s[n-n_s] = s[n-n_s-1]\}$; while the second group, $\mathbf{y}_-[n_s] := \{y[n] : n \in \mathcal{G}_-(n; n_s)\}$, is associated with the rest of n's in the set $\mathcal{G}_-(n; n_s) := \{n : s[n-n_s] = -s[n-n_s-1]\}$. For a given n_s, this partitioning into the nonoverlapping sets, $\mathcal{G}_+(n; n_s)$ and $\mathcal{G}_-(n; n_s)$, is solely determined by whether successive symbols have identical or opposite signs. The corresponding cardinalities of these two data sets are denoted by $N_t^+ := |\mathcal{G}_+(n; n_s)|$ and $N_t^- := |\mathcal{G}_-(n; n_s)|$, respectively, both of which are solely decided by the TS pattern; thus, they are independent of n_s. The signal model in (5) is then reduced to

$$y[n] = \begin{cases} A_\epsilon N_f s[n-n_s] + w[n], & y[n] \in \mathbf{y}_+[n_s] \\ A_\epsilon(N_f - 2\nu_{f,\epsilon})s[n-n_s] + w[n], & y[n] \in \mathbf{y}_-[n_s]. \end{cases} \qquad (8)$$

The results established in [10] will be helpful in our transmitter design:

Result 1 (Separability of Estimation): The MLEs of A_ϵ and $\nu_{f,\epsilon}$ can be derived from the two disjoint data sets $\mathbf{y}_+[n_s]$ and $\mathbf{y}_-[n_s]$ separately. The subset $\mathbf{y}_+[n_s]$ does not contain the acquisition parameter $\nu_{f,\epsilon}$. On the other hand, for any $y[n] \in \mathbf{y}_-[n_s]$, the channel-dependent amplitude A_ϵ and the timing offset $\nu_{f,\epsilon}$ are always coupled in a nonidentifiable manner. Estimating $\nu_{f,\epsilon}$ separately from A_ϵ maintains the optimality of both $\hat{\nu}_{f,\epsilon}$ and $\hat{A}_\epsilon$ since no useful data are disregarded. ■

Based on this separability property, timing estimation can be viewed as a conditional ML (CML) estimation problem, where the amplitude A_ϵ is treated as deterministic but unknown. Let us define $\mathcal{E}_{t,s}^+ := \sum_{n \in \mathcal{G}_+(n;n_s)} s^2[n-n_s]$ and $\mathcal{E}_{t,s}^- := \sum_{n \in \mathcal{G}_-(n;n_s)} s^2[n-n_s]$ as the symbol energies in the two TS subsets. For data-aided timing, the CML solution is obtained as follows [10].

Result 2 (GLRT-Based Synchronization): Based on the GLRT, the LLR conditioned on n_s is maximized at the MLEs of A_ϵ and $\nu_{f,\epsilon}$, and is given by

$$J(n_s; \mathbf{y}) = \left\{ \frac{\mathcal{E}_{ys}^+(n; n_s)}{\mathcal{E}_{t,s}^+} + \frac{\mathcal{E}_{ys}^-(n; n_s)}{\mathcal{E}_{t,s}^-} \right\} \qquad (9)$$

where

$$\begin{aligned} \mathcal{E}_{ys}^+(n; n_s) &:= \sum_{n \in \mathcal{G}_+(n;n_s)} y[n]s[n-n_s] \\ \mathcal{E}_{ys}^-(n; n_s) &:= \sum_{n \in \mathcal{G}_-(n;n_s)} y[n]s[n-n_s]. \end{aligned}$$

The optimum timing and channel parameters can be estimated successively: $\hat{n}_s$ first, $\hat{A}_\epsilon$ afterwards, and finally $\hat{n}_f = \hat{\nu}_{f,\epsilon}$, as

$$\hat{n}_s = \arg \max_{n_s \in [0, N-N_t]} J(n_s; \mathbf{y}) \qquad (10)$$

$$\hat{A}_\epsilon(\hat{n}_s) = \frac{\mathcal{E}_{ys}^+(n; n_s)}{N_f \mathcal{E}_{t,s}^+} \qquad (11)$$

$$\hat{n}_f(\hat{A}_\epsilon, \hat{n}_s) = \frac{N_f}{2} - \frac{\mathcal{E}_{ys}^-(n; n_s)}{2\hat{A}_\epsilon \mathcal{E}_{t,s}^-}. \qquad (12)$$

A UWB waveform is detected when the maximum LLR exceeds a threshold $\mathcal{T}_{\mathrm{FA}}$ prescribed by a desired probability of false alarms P_{FA}, i.e.,

$$J(\hat{n}_s; \mathbf{y}) \geq 2\sigma_w^2 \log_2 \mathcal{T}_{\mathrm{FA}}$$

where $\mathcal{T}_{\mathrm{FA}} := \sigma_w Q^{-1}(P_{\mathrm{FA}})$ and $Q(x) := (1/\sqrt{2\pi}) \times \int_x^\infty e^{-u^2/2} du$ is the complementary error function. ■

The resulting LLR in (9) is the average of the cross-correlation energies collected in both $\mathbf{y}_+[n_s]$ and $\mathbf{y}_-[n_s]$. Clearly, $\hat{A}_\epsilon$ in (11) is given by the cross correlation $\mathcal{E}_{ys}^+(n; n_s)$ between the input and the shifted output within the subset $\mathbf{y}_+[n_s]$, while $\hat{n}_f$ in (12) is determined by the input–output cross-correlation $\mathcal{E}_{ys}^-(n; n_s)$ within the subset $\mathbf{y}_-[n_s]$. It has also been shown in [10] that the CRBs of $\hat{A}_\epsilon$ and $\hat{n}_f$ conditioned on A_ϵ are given as

$$\mathrm{CRB}(\hat{A}_\epsilon; n_s) = \frac{\sigma_w^2}{N_f^2 \mathcal{E}_{t,s}^+} = \frac{\sigma_w^2}{N_f^2 N_t^+} \qquad (13)$$

$$\mathrm{CRB}(\hat{n}_f | A_\epsilon; n_s) = \frac{\sigma_w^2}{4A_\epsilon^2 \mathcal{E}_{t,s}^-} = \frac{\sigma_w^2}{4A_\epsilon^2 N_t^-} \qquad (14)$$

which are inversely proportional to the number of training symbols in the respective subsets $\mathcal{G}_+(n; n_s)$ and $\mathcal{G}_-(n; n_s)$. The

TABLE I
TRANSMITTER RESOURCE ALLOCATION PARAMETERS

N	total number of symbols in a burst	$\mathcal{E}$	total transmission energy for a burst
N_t^+	number of training symbols in $\mathcal{S}_+$	$\mathcal{E}_t^+$	total energy for the training subset $\mathcal{S}_+$
N_t^-	number of training symbols in $\mathcal{S}_-$	$\mathcal{E}_t^-$	total energy for the training subset $\mathcal{S}_-$
N_t	number of training symbols per burst	$\mathcal{E}_t(\mathcal{E}_s)$	total energy for training (info.) symbols
N_s	number of info. symbols per burst	$\mathcal{E}_{t,0}(\mathcal{E}_{s,0})$	unit energy for one training (info.) symbol

second equalities in (13) and (14) hold because the training symbols are taken to be binary, i.e., $s[n] \in \{\pm 1\}$, $\forall n$, leading to $\mathcal{E}_{t,s}^+ = N_t^+$ and $\mathcal{E}_{t,s}^- = N_t^-$.

For a slow-varying fading channel, we suppose that the channel $g(t)$ remains invariant over a burst of NT_s seconds but may change from burst to burst. Synchronization is thus needed for every burst. Given the burst size N and a fixed total transmission energy per burst $\mathcal{E}$, the goal of this paper is to optimally allocate the power and number of symbols per burst among the training subsets $\mathcal{G}_+(n; n_s)$ and $\mathcal{G}_-(n; n_s)$, and the information-bearing symbol set.[1] Table I lists the transmitter resource allocation parameters used throughout this paper.

III. TS DESIGN

Having built the GLRT-based synchronizers at the receiver end, it is natural to ask what is the optimum transmission format that would lead to the "best" synchronization performance? In this section, we will derive a lower bound on timing estimation to establish a pertinent performance metric based on which the optimum TS design will be developed. Specifically, given the total training resources $\mathcal{E}_t$ and N_t per burst, we seek to optimize the placement, number, and power allocation of training symbols.

Quantifying timing synchronization performance often requires overly detailed calculations that offer limited insight. A sensible performance metric for optimal TS design is the CRB of the timing offset estimator that is attainable at high SNR. Nevertheless, the CRB qualitatively reflects the comparative performance of different design choices even in the transient region (low to medium SNR); thus being useful in guiding resource allocation to minimize parameter estimation error and system performance loss. Following Result 2, the CRB for n_f conditioned on A_ϵ is given in (14), whereas A_ϵ itself is an unknown parameter whose estimate obeys the CRB given in (13). To find the unconditional CRB for n_f, we consider the joint estimation of $\boldsymbol{\theta} := [n_f \ A_\epsilon]^T$ from the LLR in (7), which is associated with a Fisher information matrix $\mathbf{F}(\boldsymbol{\theta})$ given by

$$\mathbf{F}(\boldsymbol{\theta}) := \frac{1}{2\sigma_w^2}\begin{bmatrix} -\frac{\partial^2 J}{\partial n_f^2} & -\frac{\partial^2 J}{\partial n_f \partial A_\epsilon} \\ -\frac{\partial^2 J}{\partial A_\epsilon \partial n_f} & -\frac{\partial^2 J}{\partial A_\epsilon^2} \end{bmatrix} = \begin{bmatrix} \frac{4\mathcal{E}_{t,s}^-}{\sigma_w^2}A_\epsilon^2 & f_{12}(\boldsymbol{\theta}) \\ f_{12}(\boldsymbol{\theta}) & \frac{N_f^2\mathcal{E}_{t,s}^+ + (N_f-2n_f)^2\mathcal{E}_{t,s}^-}{\sigma_w^2} \end{bmatrix} \tag{15}$$

[1]There could be some latency in the system since synchronization may not be achieved instantaneously. In this paper, because our GLRT algorithm offers a close-form timing estimator based on symbol-rate data samples, the acquisition time is negligible when compared with the symbol duration. For this reason, we ignore the effect of timing-induced latency in our resource allocation scheme.

where $f_{12}(\boldsymbol{\theta}) := (1/\sigma_w^2)(2\mathcal{E}_{ys}^-(n; n_s) - 4\mathcal{E}_{t,s}^- A_\epsilon(N_f - 2n_f))$. At the MLE $\hat{\boldsymbol{\theta}}$, it holds that $\mathcal{E}_{ys}^-(n; n_s) = \mathcal{E}_{t,s}^- \hat{A}_\epsilon(N_f - 2\hat{n}_f)$; hence, the determinant of $\mathbf{F}(\hat{\boldsymbol{\theta}})$ is

$$\left|\mathbf{F}(\hat{\boldsymbol{\theta}})\right| = \frac{4N_f^2\mathcal{E}_{t,s}^-\mathcal{E}_{t,s}^+}{\sigma_w^4}A_\epsilon^2. \tag{16}$$

Letting $[\cdot]_{ij}$ denote the (i,j)th element of a matrix, the CRBs of A_ϵ and n_f are given from (15) and (16) by

$$\begin{aligned} \mathrm{CRB}(\hat{A}_\epsilon) &= \left[\mathbf{F}^{-1}(\hat{\boldsymbol{\theta}})\right]_{22} \\ &= \frac{\left[\mathbf{F}(\hat{\boldsymbol{\theta}})\right]_{11}}{\left|\mathbf{F}(\hat{\boldsymbol{\theta}})\right|} \\ &= \frac{\sigma_w^2}{\mathcal{E}_{t,s}^+} \\ &= \frac{\sigma_w^2}{N_t^+} \end{aligned} \tag{17}$$

$$\begin{aligned} \mathrm{CRB}(\hat{n}_f) &= \left[\mathbf{F}^{-1}(\hat{\boldsymbol{\theta}})\right]_{11} \\ &= \frac{\sigma_w^2}{4\mathcal{E}_{t,s}^- A_\epsilon^2} + \frac{\sigma_w^2(N_f-2n_f)^2}{4N_f^2\mathcal{E}_{t,s}^+ A_\epsilon^2} \\ &= \frac{\sigma_w^2 N_f^2}{4N_f\mathcal{E}_t^- \mathcal{A}_\epsilon^2} + \frac{\sigma_w^2(N_f-2n_f)^2}{4N_f\mathcal{E}_t^+ \mathcal{A}_\epsilon^2} \end{aligned} \tag{18}$$

where the last equality in (18) holds because $\mathcal{E}_t^+ := \mathcal{E}_{t,0}\mathcal{E}_{t,s}^+$, $\mathcal{E}_t^- := \mathcal{E}_{t,0}\mathcal{E}_{t,s}^-$ and $A_\epsilon = \sqrt{\mathcal{E}_{t,0}/N_f}\mathcal{A}_\epsilon$. Compared with the conditional CRB $(\hat{n}_f|A_\epsilon)$ in (14), the result in (18) has an additional second term that is dependent on the acquisition offset n_f itself. The CRBs in (17) and (18) indicate the following.

1) The accuracy in estimating A_ϵ is solely decided by the cardinality of $\mathcal{G}_+(n; n_s)$. An increase in the size of this TS subset will improve the accuracy of $\hat{A}_\epsilon$.
2) The accuracy in estimating n_f is not only dependent on A_ϵ, which indicates the energy captured, but also on n_f itself. As a result, the optimum TS pattern should depend on both A_ϵ and n_f, both of which are unfortunately not available at the transmitter.

Our approach to optimizing the TS format based on whatever is available at the transmitter is to select the power, number, and placement of pilot symbols. Especially, we wish to allocate resources between the two disjoint TS subsets $\mathcal{S}_+ := \{s[n] : n \in \mathcal{G}_+(n; 0)\}$ and $\mathcal{S}_- := \{s[n] : n \in \mathcal{G}_-(n; 0)\}$, which are critical under the GLRT framework. At first glance, the CRB of n_f does not seem to favor a special ordering for $\mathcal{S}_+$ and $\mathcal{S}_-$. However, the GLRT rule seeks the MLE of A_ϵ from $\mathbf{y}_+[n_s]$

before moving on to $\mathbf{y}_-[n_s]$ for $\hat{n}_f$, which is dependent on $\hat{A}_\epsilon$. This dependence motivates one to put all $s[n] \in \mathcal{S}_+$ in the first segment of the TS (in order to ensure reliable estimation of A_ϵ) and the rest $s[n] \in \mathcal{S}_-$ in the second segment. Although such a placement itself does not affect estimation performance without being jointly considered with power or number allocation, it provides a platform for possible symbol power allocation. Different transmission energies can be allocated to these two segments of input symbols, which can be parameterized by setting $s[n] \in \{\pm 1\}$ for $n \in \mathcal{G}_+(n;0)$ and $s[n] = \{\pm\alpha\}$ for $n \in \mathcal{G}_-(n;0)$. Accordingly, the respective total symbol energies allocated to $\mathcal{S}_+$ and $\mathcal{S}_-$ are expressed by $\mathcal{E}_t^+ = \mathcal{E}_{t,0} N_t^+$ and $\mathcal{E}_t^- = \alpha^2 \mathcal{E}_{t,0} N_t^-$.

It follows from (18) that the CRB of the acquisition parameter estimator only concerns the energies allocated to the two subsets $\mathcal{S}_+$ and $\mathcal{S}_-$. For a fixed total energy $\mathcal{E}_t$, we formulate the following power allocation problem regarding the optimum values for $\mathcal{E}_t^+$ and $\mathcal{E}_t^- = \mathcal{E}_t - \mathcal{E}_t^+$, i.e.,

$$\begin{aligned}\min_{\mathcal{E}_t^+} \mathcal{L}\left(\mathcal{E}_t^+; n_f\right) &:= \mathrm{CRB}(\hat{n}_f) \\ &= \frac{\sigma_w^2 N_f^2}{4N_f\left(\mathcal{E}_t - \mathcal{E}_t^+\right)\mathcal{A}_\epsilon^2} + \frac{\sigma_w^2 (N_f - 2n_f)^2}{4N_f \mathcal{E}_t^+ \mathcal{A}_\epsilon^2}. \quad (19)\end{aligned}$$

Substituting n_f by $N_f - n_f$ in (19) does not change the objective function; thus, we can henceforth consider $n_f \le N_f/2$ and generalize our results to $n_f > N_f/2$ by simply replacing n_f by its mirror point $N_f - n_f \in [0, N_f/2]$ around the folding pivot $N_f/2$. The first-order derivative of (19) with respect to $\mathcal{E}_t^+$ is given by

$$\begin{aligned}\frac{\partial \mathcal{L}\left(\mathcal{E}_t^+; n_f\right)}{\partial \mathcal{E}_t^+} = \frac{\sigma_w^2}{4N_f \mathcal{A}_\epsilon^2} &\frac{\left[2n_f \mathcal{E}_t^+ + \mathcal{E}_t(N_f - 2n_f)\right]}{\left(\mathcal{E}_t^+\right)^2\left(\mathcal{E}_t - \mathcal{E}_t^+\right)^2} \\ &\times \left[2(N_f - n_f)\mathcal{E}_t^+ - \mathcal{E}_t(N_f - 2n_f)\right] \quad (20)\end{aligned}$$

that, when set to zero, yields

$$\left(\mathcal{E}_t^+\right)_{\mathrm{opt}} = \mathcal{E}_t \frac{N_f - 2n_f}{2(N_f - n_f)} \le \frac{\mathcal{E}_t}{2}. \quad (21)$$

Because $\left(\mathcal{E}_t^+\right)_{\mathrm{opt}}$ is monotonically decreasing with n_f and is upper bounded by $\mathcal{E}_t/2$ for all n_f, we deduce that n_f estimation should be allocated at least as much power as channel amplitude estimation.

When the energies $\mathcal{E}_t^+$ and $\mathcal{E}_t^-$ are optimally allocated according to (21), the objective function in (19) reaches the minimum, i.e.,

$$\begin{aligned}\mathrm{CRB}(\hat{n}_f)_{\mathrm{opt}} &:= \mathcal{L}\left(\left(\mathcal{E}_t^+\right)_{\mathrm{opt}}; n_f\right) \\ &= \frac{\sigma_w^2 (N_f - n_f)^2}{N_f \mathcal{E}_t \mathcal{A}_\epsilon^2} \\ &\le \frac{\sigma_w^2 N_f}{\mathcal{E}_t \mathcal{A}_\epsilon^2} \quad (22)\end{aligned}$$

where the last equality holds when $n_f = 0$ and serves as a loose performance bound for $\hat{n}_f$. This result directly links acquisition performance to the total energy $\mathcal{E}_t$ of all training symbols as well as the receiver's energy capture parameter $\mathcal{A}_\epsilon$ in the presence of tracking offset ϵ and TH.

Knowing the optimum total energy for each of the two subsets $\mathcal{S}_+$ and $\mathcal{S}_-$, we seek the optimum number allotment for these two subsets and the optimum energy allocation to each individual symbol. Within each subset, the energy of each symbol is given by $\mathcal{E}_{t,0}^+ := \mathcal{E}_t^+/N_t^+ = \mathcal{E}_{t,0}$ in $\mathcal{S}_+$, and $\mathcal{E}_{t,0}^- := \mathcal{E}_t^-/N_t^- = \alpha^2 \mathcal{E}_{t,0}$ in $\mathcal{S}_-$. As a result, $\alpha^2 = \mathcal{E}_{t,0}^-/\mathcal{E}_{t,0}^+$ represents the energy allocation factor between the two subsets. The total energy allocation can be expressed as $\mathcal{E}_t^+/\mathcal{E}_t = N_t^+/(N_t^+ + \alpha^2 N_t^-)$. Meanwhile, the total number of training symbols is $N_t = N_t^+ + N_t^- + 1$, where the extra 1 bit refers to $s[0]$, which does not belong to either $\mathcal{S}_+$ or $\mathcal{S}_-$ because $s[-1]$ is not used in timing. Accordingly, both power allocation and size allocation for each set can be deduced from (21) by obeying the optimum ratio $\left(\mathcal{E}_t^+/\mathcal{E}_t\right)_{\mathrm{opt}}$. The following propositions follow readily from (21).

Proposition 1 (Training Number Allocation): For a fixed energy ratio α^2, the optimum number of training symbols allocated to each subset $\mathcal{S}_+$, $\mathcal{S}_-$ is determined by

$$\begin{aligned}\left(\frac{N_t^+}{N_t}\right)_{\mathrm{opt}} &= \frac{\alpha^2 \left(\frac{\mathcal{E}_t^+}{\mathcal{E}_t}\right)_{\mathrm{opt}}}{1 + (\alpha^2 - 1)\left(\frac{\mathcal{E}_t^+}{\mathcal{E}_t}\right)_{\mathrm{opt}}} \\ &= 1 - \frac{N_f}{N_f + \alpha^2(N_f - 2n_f)}. \quad (23)\end{aligned}$$

We infer from Proposition 1 that $\left(N_t^+/N_t^-\right)_{\mathrm{opt}} = \alpha^2(N_f - 2n_f)/N_f$, which decreases as n_f increases. This means that a larger timing offset requires a larger number of training symbols to be allocated to the set $\mathcal{S}_-$ of training symbols with alternating signs.

Proposition 2 (Training Energy Allocation): For a fixed assignment N_t^+ out of N_t, the energy ratio α^2 that minimizes the acquisition CRB is

$$(\alpha^2)_{\mathrm{opt}} = \frac{\mathcal{E}_t - \left(\mathcal{E}_t^+\right)_{\mathrm{opt}}}{\left(\mathcal{E}_t^+\right)_{\mathrm{opt}}} \frac{N_t^+}{N_t^-} = \frac{N_f}{N_f - 2n_f} \frac{N_t^+}{N_t - N_t^+}. \quad (24)$$

We deduce from Proposition 2 that the optimum α^2 increases when either N_t^+ or n_f increases, which suggests that a higher level of per-symbol energy $\mathcal{E}_{t,0}^- = \alpha^2 \mathcal{E}_{t,0}^+$ should be assigned to $\mathcal{S}_-$ to compensate for a smaller size of $\mathcal{S}_-$ or a larger timing offset n_f.

Propositions 1 and 2 are useful when either energy or number assignments to the two sets $\mathcal{S}_+$ and $\mathcal{S}_-$ are fixed due to system operating constraints. When a system permits flexible TS design in both power and number, it is possible to find the optimal solution to the (N_t^+, α^2) pair by alternating optimization using Propositions 1 and 2. To reach directly a joint optimization solution, we pose the following TS design question: given the total symbol energy $\mathcal{E}_t = \mathcal{E}_{t,0} N_t^+ + \alpha^2 \mathcal{E}_{t,0} N_t^-$ and the total number of symbols $N_t = N_t^+ + N_t^-$, what are the optimum values for

α and N_t^+ that minimize the acquisition error expressed by the CRB $(\hat{n}_f)$? Mathematically, this problem is expressed as

$$\min_{\alpha^2\geq 0, N_t^+\leq N_t} \text{CRB}(\hat{n}_f) = \frac{\sigma_w^2 N_f^2}{4N_f\alpha^2\mathcal{E}_{t,0}\left(N_t - N_t^+\right)\mathcal{A}_\epsilon^2} + \frac{\sigma_w^2(N_f-2n_f)^2}{4N_f\mathcal{E}_{t,0}N_t^+\mathcal{A}_\epsilon^2} \quad (25)$$

$$\text{s.t.} \quad \alpha^2\mathcal{E}_{t,0}\left(N_t - N_t^+\right) + \mathcal{E}_{t,0}N_t^+ = \mathcal{E}_t. \quad (26)$$

This objective function is the same as that in (19). In addition, an energy constraint is imposed, where $\mathcal{E}_t/\mathcal{E}_{t,0}$ is considered fixed. Using (21), the joint optimization strategy under the energy constraint is summarized below.

Proposition 3 (Joint Training Resource Allocation): Given the total number of training symbols N_t, the total training transmission energy $\mathcal{E}_t$, and a fixed $\mathcal{E}_t/\mathcal{E}_{t,0}$, the joint power and number allocation results are

power allocation

$$(\alpha^2)_{\text{opt}} = \frac{\frac{N_f\mathcal{E}_t}{\mathcal{E}_{t,0}}}{2(N_f-n_f)\left(N_t - \frac{\mathcal{E}_t}{\mathcal{E}_{t,0}}\right) + \frac{N_f\mathcal{E}_t}{\mathcal{E}_{t,0}}} \quad (27)$$

number allocation

$$\left(N_t^+\right)_{\text{opt}} = \frac{(N_f-2n_f)}{2N_f-2n_f}\frac{\mathcal{E}_t}{\mathcal{E}_{t,0}}. \quad (28)$$

Observe from Propositions 1–3 that both the power and number allocation on training symbols rely on the unknown n_f. To shed light on a possible practical TS design, we plot in Fig. 1 the objective function $\mathcal{L}(\mathcal{E}_t^+; n_f)$ in (19) versus $\mathcal{E}_t^+$ for various n_f. Consistent to (21), the optimum $\mathcal{E}_t^+$ should always take less than half of $\mathcal{E}_t$ for any n_f. Although $(\mathcal{E}_t^+)_{\text{opt}}$ is dependent on n_f, the $\mathcal{L}(\mathcal{E}_t^+; n_f)$ curves are relatively flat around $(\mathcal{E}_t^+)_{\text{opt}}$ regardless of n_f but degrade drastically when far away from $(\mathcal{E}_t^+)_{\text{opt}}$. Specifically, $\mathcal{L}(\mathcal{E}_t^+; n_f)$ seems to be insensitive to $\mathcal{E}_t^+ \in [0.3, 0.5)$ for all possible $n_f \in [0, N_f - 1]$. Meanwhile, (21) implies that $(\mathcal{E}_t^+)_{\text{opt}} \in [0.3, 0.5)$ corresponds to $n_f \in (0, 2/7]N_f$. This suggests that a practical TS design can be implemented based on a nominal value of n_f chosen within a robust region $n_f \in (0, 2/7]N_f$ followed by the power and number allocation suggested in Propositions 1–3. For example, choosing a nominal $n_f = N_f/4$ yields $(N_t^+)_{\text{opt}} = 1/3$ and $(\alpha^2)_{\text{opt}} = 2/((3N_t/(\mathcal{E}_t/\mathcal{E}_{t,0})) - 1)$ based on Proposition 3. Without resorting to the actual n_f, such a design is not only practical but also very close to the optimum.

In our results so far, we considered a fixed average energy ratio $\mathcal{E}_t/\mathcal{E}_{t,0}$. Since we are only concerned with training for timing estimation, the absolute value of $\mathcal{E}_{t,0}$ is irrelevant in allocating resources for TS design, whereas α^2 is relevant. On the other hand, the SNR of the TS is related to $\mathcal{E}_{t,0}/\sigma_w^2$, which can be used for optimum resource allocation when the detection quality and the rate of information-bearing symbols are to be taken into account as well. Next, we pursue optimal resource allocation between training and information-bearing symbols.

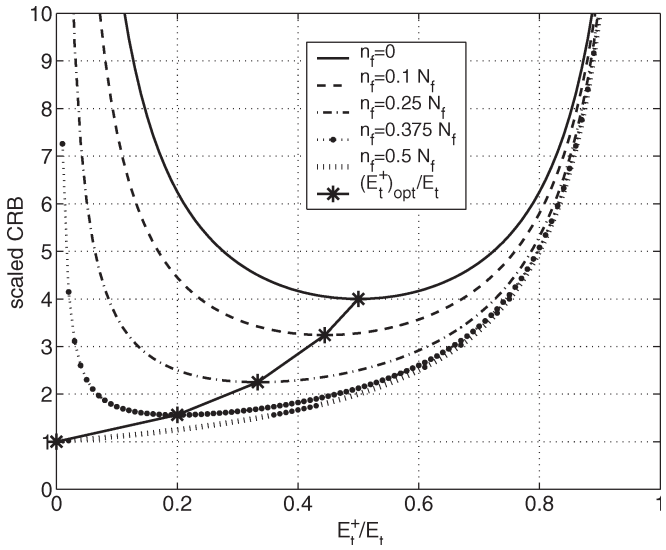

Fig. 1. Objective function in (19) versus $\mathcal{E}_t^+/\mathcal{E}_t$ parameterized by n_f : $\alpha^2 = 1$, $N_t^+ = (\mathcal{E}_t^+/\mathcal{E}_t)N_t$.

IV. System-Level Transmission Resource Allocation

A good TS design leads to improved acquisition accuracy, which in turn benefits symbol detection performance during the information conveying phase. For each transmission burst of NT_s seconds, we suppose that it includes N_t training symbols and $N_s := N - N_t$ symbols for conveying information messages. It is indicated by (22) that the timing acquisition mean-square error (MSE) decreases monotonically as $\mathcal{E}_t$ increases. On the other hand, for a fixed total transmission energy per burst $\mathcal{E} = \mathcal{E}_t + \mathcal{E}_s$, the energy assigned to information symbols $\mathcal{E}_s$ decreases as $\mathcal{E}_t$ increases. Similarly, for a fixed burst size N, the information rate decreases as N_t increases. It is not obvious what the optimum $\mathcal{E}_t$ and N_t are. In this section, we discuss the optimum transmitter design in terms of the power, number, and placement of training symbols and information-bearing symbols per burst. The goal is to design the transmission format that optimizes not only the timing acquisition performance but also the information rate.

A. Effective SNR and Average Channel Capacity

To capture the information rate, we will use the average capacity C as the performance metric. The overall system can be viewed as a binary symmetric channel (BSC) with a transition probability P that depends on both the propagation channel and the receiver structure and that provides a measure of both performance and information rate achievable by our UWB receiver with timing acquisition, correlation reception, and information symbol detection.

To evaluate the average capacity C, we start from the received waveform during the information conveying phase. After timing acquisition, we assume that the symbol-level timing offset n_s has been accurately estimated, and set $n_s = 0$ without loss of generality. The frame-level timing estimation is given by $\hat{n}_f$ and the estimation error is denoted as $\tilde{n}_f := n_f - \hat{n}_f$. The

remaining timing offset that affects detection of information-bearing symbols is given by $\tau_s = \tilde{n}_f T_f + \epsilon$. As a result, the received signal corresponding to the nth symbol-long observation $[nT_s, (n+1)T_s)$, $n = 0, \ldots, N_s - 1$, can be represented by [cf. (2)]

$$r_n(t) = \sqrt{\frac{\mathcal{E}_{s,0}}{N_f}} \{s[n-1] g_s(t + T_s - \tilde{n}_f T_f - \epsilon) + s[n] g_s(t - \tilde{n}_f T_f - \epsilon)\} + w(t), \qquad t \in [0, T_s). \tag{29}$$

Let us now suppose that the channel can be perfectly estimated after timing acquisition so that the effect of timing estimation can be separated from that of channel estimation. Subject to the residual timing offset τ_s, the estimated channel is conceptually equivalent to the signal component in (29) under training $s[n] = s[n-1] = 1$, which leads to a T_s-long correlation template

$$h_{rs}(t) = g_s(t - \tilde{n}_f T_f - \epsilon) + g_s(t + T_s - \tilde{n}_f T_f - \epsilon), \qquad t \in [0, T_s). \tag{30}$$

Apparently, $h_{rs}(t)$ is nothing but the received symbol-waveform $g_s(t) = \sum_{j=0}^{N_f - 1} g(t - jT_f - c_j T_c)$ after being circularly shifted by τ_s to confine it within the range $[0, T_s]$. The correlator yields discrete-time output samples $y[n] := \int_0^{T_s} r_n(t) h_{rs}(t) dt$ at the symbol rate. Noting that the composite channel $g(t)$ has a finite nonzero support on $[0, T_f)$, $y[n]$ can be simplified from (29) and (30) to

$$\begin{aligned} y[n] &= \sqrt{\frac{\mathcal{E}_{s,0}}{N_f}} s[n] \int_{\tilde{n}_f T_f + \epsilon}^{T_s} g_s(t - \tilde{n}_f T_f - \epsilon) h_{rs}(t) dt \\ &\quad + \sqrt{\frac{\mathcal{E}_{s,0}}{N_f}} s[n-1] \\ &\quad \times \int_0^{\tilde{n}_f T_f + \epsilon} g_s(t + T_s - \tilde{n}_f T_f - \epsilon) h_{rs}(t) dt + w[n] \\ &= \sqrt{\frac{\mathcal{E}_{s,0}}{N_f}} \mathcal{R}_g \left((N_f - \tilde{n}_f - \lambda_{g,\epsilon}) s[n] \right. \\ &\qquad \left. + (\tilde{n}_f + \lambda_{g,\epsilon}) s[n-1] \right) + w[n] \end{aligned} \tag{31}$$

where $\mathcal{R}_g := \int_0^{T_f} g^2(t) dt$ and $\lambda_{g,\epsilon} := (1/\mathcal{R}_g) \int_{T_f - \epsilon}^{T_f} g^2(t) dt$. The noise $w[n]$ is a Gaussian random variable with zero mean and variance $\sigma_w^2 = (\mathcal{N}_o/2) \mathcal{R}_g N_f$. Equation (31) agrees with the input–output signal model (4) under mistiming, where the impact of the frame-level timing offset appears as an effective channel amplitude. As a special case of (4) with the correlation template being $p_{rs}(t) = h_{rs}(t)$, we observe from (31) that $\mathcal{A}_\epsilon = \mathcal{R}_g$ and $\tilde{\nu}_{f,\epsilon} := \tilde{n}_f + \lambda_{g,\epsilon}$. Note that $\mathcal{R}_g$ contains all the channel energy through optimum maximum ratio combining. Similar to (8), (31) can be expressed by

$$y[n] = \begin{cases} \sqrt{\frac{\mathcal{E}_{s,0}}{N_f}} \mathcal{R}_g N_f s[n] + w[n], & s[n] = s[n-1] \\ \sqrt{\frac{\mathcal{E}_{s,0}}{N_f}} \mathcal{R}_g \left(N_f - 2(\tilde{n}_f + \lambda_{g,\epsilon}) \right) \\ \quad \times s[n] + w[n], & s[n] = -s[n-1]. \end{cases} \tag{32}$$

Generalizing the CRB result (22) in the TS design, the MSE of $\tilde{\nu}_{f,\epsilon}$ is bounded by $\sigma^2_{\tilde{\nu}_{f,\epsilon}} = \sigma_w^2 N_f / (\mathcal{A}_\epsilon^2 \mathcal{E}_t) = \sigma_w^2 N_f / (\mathcal{R}_g^2 \mathcal{E}_t) = N_f^2 (\mathcal{N}_o/2) / (\mathcal{E}_t \mathcal{R}_g)$ when the optimum TS design in Section III is in effect. Meanwhile, the timing ambiguity $\lambda_{g,\epsilon}$, its mean, and MSE are all bounded; that is, $\lambda_{g,\epsilon} \in [0,1]$, $\bar{\lambda}_{g,\epsilon} := E_\epsilon\{\lambda_{g,\epsilon}\} \in [0,1]$, and $\sigma_\epsilon^2 := E_\epsilon\{|\lambda_{g,\epsilon} - \bar{\lambda}_{g,\epsilon}|^2\} \in [0,1]$. The MSE of the timing mismatch $\hat{n}_f$ itself is then given by

$$\begin{aligned} \sigma^2_{\tilde{n}_f} &= E_{\tilde{\nu}_{f,\epsilon},\epsilon} \left\{ |\tilde{\nu}_{f,\epsilon} - \lambda_{g,\epsilon} - E\{\tilde{\nu}_{f,\epsilon} - \lambda_{g,\epsilon}\}|^2 \right\} \\ &= \sigma^2_{\tilde{\nu}_{f,\epsilon}} + \sigma_\epsilon^2 = \frac{\sigma_w^2 N_f}{\mathcal{R}_g^2 \mathcal{E}_t} + \sigma_\epsilon^2. \end{aligned} \tag{33}$$

Equation (33) shows that as $\mathcal{E}_t$ increases, the timing acquisition MSE decreases monotonically. On the other hand, for a fixed total transmission energy per burst $\mathcal{E} = \mathcal{E}_t + \mathcal{E}_s$, the energy assigned to information symbols $\mathcal{E}_s$ decreases as $\mathcal{E}_t$ increases. To strike a balance between the timing MSE and the information rate, we will use the average capacity as the performance metric for transmission power allocation. To this end, we first find the effective SNR ρ_{eff} of each information-bearing symbol.

Reexamining the discrete-time signal model (31), we partition it into a signal component $\tilde{s}[n] := \sqrt{\mathcal{E}_{s,0}/N_f} \mathcal{R}_g (N_f - \tilde{n}_f - \lambda_{g,\epsilon}) s[n]$ and a noise component $\tilde{w}[n] := \sqrt{\mathcal{E}_{s,0}/N_f} \mathcal{R}_g (\tilde{n}_f + \lambda_{g,\epsilon}) s[n-1] + w[n]$. Recognizing that the ML timing acquisition is unbiased, i.e., $E\{\tilde{n}_f\} = 0$, the signal component energy is given by

$$E_{\tilde{n}_f,\epsilon} \left\{ |\tilde{s}[n]|^2 \right\} = \left(\frac{\mathcal{E}_{s,0} \mathcal{R}_g^2}{N_f} \right) \left[\sigma^2_{\tilde{n}_f} + \sigma_\epsilon^2 + (N_f - \bar{\lambda}_{g,\epsilon})^2 \right]. \tag{34}$$

Similarly, the noise component energy is given by

$$E_{\tilde{n}_f,\epsilon} \left\{ |\tilde{w}[n]|^2 \right\} = \sigma_w^2 + \left(\frac{\mathcal{E}_{s,0} \mathcal{R}_g^2}{N_f} \right) \left[\sigma^2_{\tilde{n}_f} + \sigma_\epsilon^2 + \bar{\lambda}^2_{g,\epsilon} \right]. \tag{35}$$

Putting things together, the effective SNR is

$$\rho_{\text{eff}} = \frac{E_{\tilde{n}_f,\epsilon} \left\{ |\tilde{s}[n]|^2 \right\}}{E_{\tilde{n}_f,\epsilon} \left\{ |\tilde{w}[n]|^2 \right\}} = \frac{\sigma^2_{\tilde{n}_f} + \sigma_\epsilon^2 + (N_f - \bar{\lambda}_{g,\epsilon})^2}{\sigma^2_{\tilde{n}_f} + \sigma_\epsilon^2 + \bar{\lambda}^2_{g,\epsilon} + \frac{N_f^2 \mathcal{N}_o}{(2\mathcal{E}_{s,0} \mathcal{R}_g)}}. \tag{36}$$

It follows from (36) that the effective SNR is upper bounded by $\rho_{\text{eff}} = 2\mathcal{E}_{s,0} \mathcal{R}_g / \mathcal{N}_o$ when perfect timing is known deterministically, i.e., $\sigma^2_{\tilde{n}_f} = 0$, $\bar{\lambda}_{g,\epsilon} = 0$, and $\sigma_\epsilon^2 = 0$. Here, $\mathcal{R}_g$ represents

the energy capture capability of the detector and $\mathcal{E}_{s,0}\mathcal{R}_g$ is the effective received signal energy per symbol. In the presence of timing offset, the effect of tracking errors not only shows up in σ_ϵ^2 but also affects the energy capture through $\bar{\lambda}_{g,\epsilon}$. The acquisition error affects ρ_{eff} via $\sigma_{\tilde{n}_f}^2$.

To link capacity with acquisition MSE, we recall that $\mathcal{E}_t$ determines the timing MSE, which affects the overall system performance. The achievable information rate of the underlying system can be measured by the average channel capacity. For a BSC channel, the mutual information $I(\hat{s}[n], g(t); s[n])$ between $s[n]$ and $\hat{s}[n]$ depends not only on the channel $g(t)$ but also on the transition probability P. Recalling that every N_s out of N symbols are information conveying, the average channel capacity is maximized by equal-powered information symbols, which corresponds to [14]

$$\begin{aligned} C &= \frac{1}{N}\max_{P(s[n])}\sum_{n=0}^{N_s-1} I\left(\hat{s}[n], g(t); s[n]\right) \\ &= \frac{N_s}{N} E_g\left\{P\log_2 P + (1-P)\log_2(1-P) + 1\right\} \end{aligned} \tag{37}$$

where the probability that an input symbol $s[n]$ is erroneously decoded is determined by its corresponding effective SNR given by

$$\begin{aligned} P &= Q(\sqrt{\rho_{\text{eff}}}) \\ &= Q\left(\sqrt{\frac{2\mathcal{E}_{s,0}\mathcal{R}_g}{\mathcal{N}_o}\frac{\sigma_{\tilde{n}_f}^2 + \sigma_\epsilon^2 + (N_f - \bar{\lambda}_{g,\epsilon})^2}{\left(\frac{2\mathcal{E}_{s,0}\mathcal{R}_g}{\mathcal{N}_o}\right)\left(\sigma_{\tilde{n}_f}^2 + \sigma_\epsilon^2 + \bar{\lambda}_{g,\epsilon}^2\right) + N_f^2}}\right). \end{aligned} \tag{38}$$

When $\sigma_{\tilde{n}_f}^2$ decreases, the effective SNR increases as long as the received energy satisfies the weak condition

$$\frac{2\mathcal{E}_{s,0}\mathcal{R}_g}{\mathcal{N}_o} > \frac{1}{N_f(N_f - 2\bar{\lambda}_{g,\epsilon})}. \tag{39}$$

Thus, minimizing the timing MSE also maximizes the average capacity.

B. Optimizing Over the Energy Allocation

Let us define the energy allocation factor $\beta := \mathcal{E}_s/\mathcal{E} \in (0,1)$ as the fraction of the total transmission energy per burst that is allocated to information symbols. Accordingly, $\mathcal{E}_t = (1-\beta)\mathcal{E}$. Also defining $\rho := (\mathcal{E}/N)/(\mathcal{N}_o/2)$ as the nominal SNR per received symbol, we substitute (33) into (36) to reach a more convenient form for ρ_{eff}, i.e.,

$$\rho_{\text{eff}}(\beta) = \frac{\frac{1}{N\rho(1-\beta)} + \frac{\mathcal{R}_g\left(2\sigma_\epsilon^2 + \left(N_f^2 - \bar{\lambda}_{g,\epsilon}\right)^2\right)}{N_f^2}}{\frac{N_s}{N\rho\beta} + \frac{1}{N\rho(1-\beta)} + \frac{\mathcal{R}_g\left(2\sigma_\epsilon^2 + \bar{\lambda}_{g,\epsilon}^2\right)}{N_f^2}}. \tag{40}$$

Differentiating ρ_{eff} with respect to β yields the optimum power allocation factor β^* as

$$\beta^* = \frac{N_s - \sqrt{N_s\frac{N_f^2 - 2N_f\bar{\lambda}_{g,\epsilon} - N_s + 1}{2\sigma_\epsilon^2 + (N_f - \bar{\lambda}_{g,\epsilon})^2} - \frac{N_f^2 N_s\left(2\sigma_\epsilon^2 + \bar{\lambda}_{g,\epsilon}^2\right)}{N\rho\mathcal{R}_g\left(2\sigma_\epsilon^2 + (N_f - \bar{\lambda}_{g,\epsilon})^2\right)^2}}}{N_s - \frac{N_f^2 - 2N_f\bar{\lambda}_{g,\epsilon}}{2\sigma_\epsilon^2 + (N_f - \bar{\lambda}_{g,\epsilon})^2}}. \tag{41}$$

When $\bar{\lambda}_{g,\epsilon}, \sigma_\epsilon^2 \le 1 \ll N_f$, the optimum β^* reduces to

$$\beta^* = \frac{\sqrt{N_s}}{\sqrt{N_s}+1}\frac{\sqrt{N_s} - \sqrt{1 - \frac{N_s - 1}{N_f^2} - \frac{1}{N\rho\mathcal{R}_g}}}{\sqrt{N_s} - 1}. \tag{42}$$

Furthermore, when the total receive SNR satisfies $N\rho\mathcal{R}_g \gg 1$, β^* can be simplified to

$$\beta^* \approx \begin{cases} \frac{\sqrt{N_s}}{\sqrt{N_s}+1}, & N_s \ll N_f^2 \\ 1 - \sqrt{\frac{1}{N_s} - \frac{1}{N_f^2}}, & 1 \ll N_s < N_f^2. \end{cases} \tag{43}$$

Proposition 4 (Energy Allocation Per Burst): With a fixed burst size N, fixed number of pilot symbols per burst N_s, and fixed total transmission energy per burst $\mathcal{E}$, the optimum energy allocation factor $\beta := \mathcal{E}_s/\mathcal{E}$ that maximizes C is given by β^* in (41)–(43).

Knowing the energy allocated to the training and information symbol sets, the average training and information energies per symbol are given, respectively, by $\mathcal{E}_{s,0} = \beta^*\mathcal{E}/N_s$ and $\mathcal{E}_{t,0} = (1-\beta^*)\mathcal{E}/(N - N_s)$. As a result, the optimum energy ratio per symbol can be deduced from Proposition 4 as (assuming $N\rho\mathcal{R}_g \gg 1$):

$$\left(\frac{\mathcal{E}_{s,0}}{\mathcal{E}_{t,0}}\right)_{\text{opt}} = \begin{cases} \frac{N - N_s}{\sqrt{N_s}}, & N_s \ll N_f^2 \\ \frac{N - N_s}{\sqrt{N_s}}\left(\frac{1}{\sqrt{1 - \frac{N_s}{N_f^2}}} - \frac{1}{\sqrt{N_s}}\right), & 1 \ll N_s < N_f^2. \end{cases} \tag{44}$$

This indicates that the per-symbol energies for training and information symbols to maximize C should not be equal in general. On the other hand, transmissions with nonconstant envelopes may reduce the power amplification efficiency of nonlinear amplifiers at the receiver front-end.

C. Optimizing Over the Number Allocation

Inspection of (37) and (38) reveals that for a fixed N, the capacity C depends on N_s, $\mathcal{E}_s$, $\mathcal{E}_t$, but is independent of N_t. Meanwhile, the timing acquisition MSE in (33) is determined by $\mathcal{E}_t$, which does not directly concern N_t either. The optimum number allocation boils down to finding the optimum N_s that maximizes C—a task independent of the timing MSE minimization as long as $\mathcal{E}_t$ remains fixed.

We note that when N_s increases, the effective ρ_{eff} decreases as $\mathcal{E}_{s,0} = \mathcal{E}_s/N_s$ decreases, reducing the per-symbol mutual information $I(\hat{s}[n], g(t); s[n])$ at a sublinear rate. On the other hand, the capacity is directly proportional to N_s. Overall, the average channel capacity monotonically increases as N_s increases. In fact, it can be shown that the first-order derivative

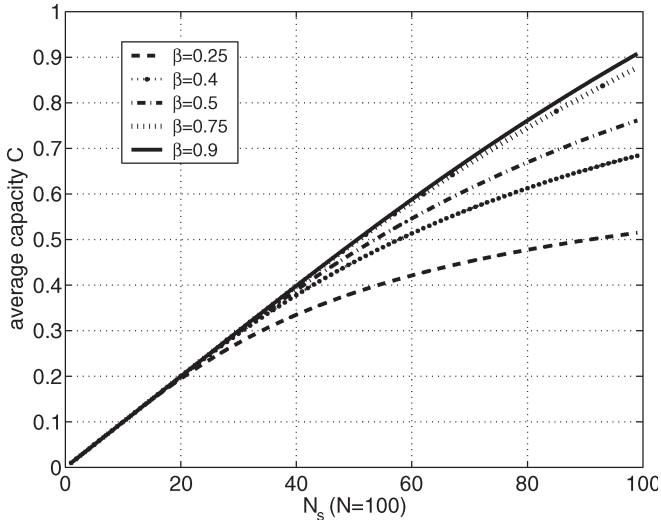

Fig. 2. Average capacity versus N_s for various β.

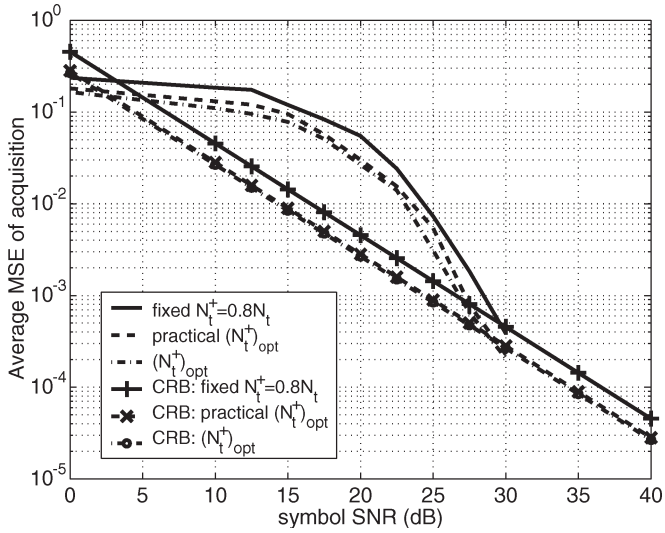

Fig. 3. Acquisition MSE under various TS number allocation N_t^+/N_t.

of C with respect to N_s, treating N, $\mathcal{E}$, and $\mathcal{E}_t$ as constants, is always positive. In Fig. 2, the average capacity C is plotted versus N_s/N for various β values using the parameters $N = 100$, $N_f = 50$, and $\rho = 10$ dB. Regardless of β, the capacity curve monotonically increases as N_s increases; hence, it is always preferable to set N_s as large as possible. On the other hand, timing acquisition requires a minimum of three training bits, that is, $N_t^+ = 1$, $N_t^- = 1$, and $N_t = N_t^+ + N_t^- + 1 = 3$. Insofar as capacity is concerned, this implies that all the training transmission energy $\mathcal{E}_t$ should be distributed to the smallest possible number of symbols. The following proposition on number allocation is in order.

Proposition 5 (Optimal Number of Pilots Per Burst):: For a given burst size $N = N_s + N_t$, information energy $\mathcal{E}_s$, and training energy $\mathcal{E}_t$, the number of information symbols N_s that maximizes the average capacity C is given by

$$N_s^* = N - 3. \tag{45}$$

D. Optimizing Equal-Powered Pilot and Information Symbols

In order to maintain a transmission where all pulses have the same amplitude for the convenience of power amplification, it may be desirable to set $\mathcal{E}_{t,0} = \mathcal{E}_{s,0}$. Under this condition, we have $\mathcal{E}_{t,0} = \mathcal{E}_{s,0} = \mathcal{E}/N$; thus, $\beta = N_s/N$ and $(1-\beta) = N_t/N$. Since the number allocation is no longer independent of the information and training energies $\mathcal{E}_t$ and $\mathcal{E}_s$, the optimization of N_s is coupled with energy allocation. The effective SNR is now given by

$$\rho_{\text{eff}}(N_s) = \frac{\frac{1}{\rho(N-N_s)} + \frac{\mathcal{R}_g\left(2\sigma_\epsilon^2 + (N_f - \bar{\lambda}_{g,\epsilon})^2\right)}{N_f^2}}{\frac{1}{\rho} + \frac{1}{\rho(N-N_s)} + \frac{\mathcal{R}_g\left(2\sigma_\epsilon^2 + \bar{\lambda}_{g,\epsilon}^2\right)}{N_f^2}}. \tag{46}$$

Correspondingly, the transition probability is $P(N_s) = Q(\sqrt{\rho_{\text{eff}}(N_s)})$ and the average capacity C becomes a function of N_s as

$$C(N_s) = \frac{N_s}{N} E\left\{P(N_s)\log_2 P(N_s) + (1-P(N_s))\log_2(1-P(N_s)) + 1\right\}. \tag{47}$$

Putting (46) and (47) together, we may resort to numerical optimization tools such as the fmin.m function in MATLAB's optimization toolbox to search for the optimum N_s^* under the equal-power condition.

Proposition 6 (Joint Resource Allocation Per Burst): For constant-envelope transmissions with fixed ρ and burst size N, the number of information symbols N_s and the corresponding $\beta = N_s/N$ that maximize the capacity C can be numerically solved by maximizing (47).

We now conclude this section with a final remark on the unknown tracking-induced parameters σ_ϵ^2 and $\bar{\lambda}_{g,\epsilon}$. Note that $\lambda_{g,\epsilon} = (1/\mathcal{R}_g)\int_{T_f-\epsilon}^{T_f} g^2(t)dt$ depends on the channel $g(t)$ only; thus, its statistic averages, σ_ϵ^2 and $\bar{\lambda}_{g,\epsilon}$, can be measured off-line from the channel itself, independent of data transmissions. Furthermore, since both parameters are bounded by 1, their impact on transmission resource allocation is trivial as long as $N_f \gg 1$.

V. Simulations

In the simulations, we test the overall system efficiency with and without optimum TS design. In all cases, the random channels are generated according to the dense multipath model in [15] and [16] with transmitter parameters $T_p = 1$ ns, $T_f = 100$ ns, and $N_f = 50$, and channel parameters $\Gamma = 30$ ns, $\gamma = 5$ ns, $1/\Lambda = 2$ ns, and $1/\lambda = 0.5$ ns.

The analytical MSE bounds have been depicted in Fig. 1, where optimum ML timing synchronizers are used for different TS patterns. At $\alpha^2 = 1$, we have $\mathcal{E}_t^+ = (N_t^+/N_t)\mathcal{E}_t$, and the performance advantage of using an optimum TS design $(N_t^+)_{\text{opt}}$ over a fixed design N_t^+ is shown by the MSE gap between $\mathcal{L}(N_t^+; n_f)$ and $\mathcal{L}((N_t^+)_{\text{opt}}; n_f)$, depicted by the analytical MSE bounds in Fig. 1. The gap is more pronounced at the edges and less noticeable when N_t^+ is close to the center of $N_t/2$. This observation is verified by simulations over 500 random channel realizations in Fig. 3. Timing offsets n_f are randomly generated between $[0, N_f/2]$ for $N_t = 100$. The TS patterns tested include a fixed TS design with $N_t^+ = 0.8N_t$, a practical TS design with a nominal $n_f = N_f/4$, and the

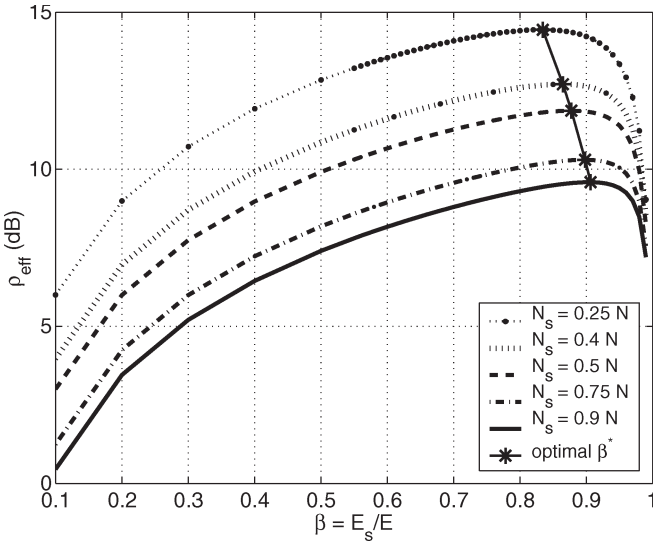

Fig. 4. Objective function for optimizing power allocation factor β.

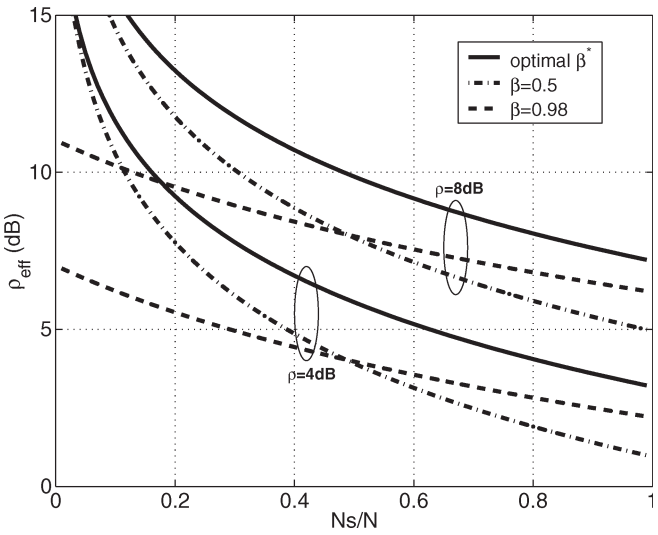

Fig. 5. Comparison of average capacity for various power allocation schemes.

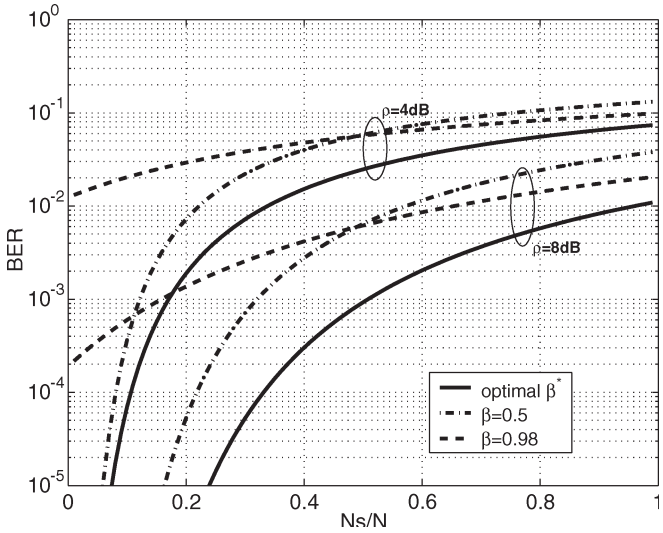

Fig. 6. Comparison of average BER for various power allocation schemes.

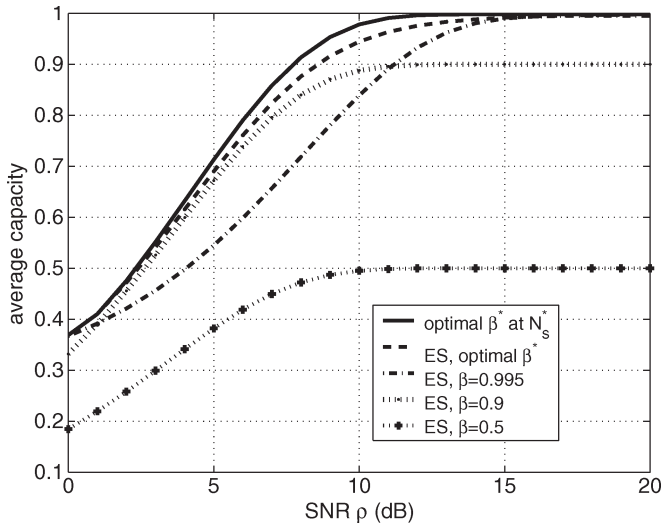

Fig. 7. Comparison of average capacity for various number allocation under the condition of equal per-symbol powers.

optimum TS using known n_f, which serves as the performance bound. The timing accuracy of our practical TS design is very close to the optimum bound, while there is a noticeable gap between the fixed-numbered TS and the optimum one. Although the timing performance is relatively insensitive to N_t^+/N_t in a broad range, this does not mean that a TS with comparable numbers of 1's and -1's is a robust design: the same number of 1's and -1's can be arranged differently to yield different N_t^+ and N_t^- values, depending on the TS pattern.

At the system level, we compare the average channel capacity of our optimum power and number allocation results. Fig. 4 depicts the optimum β^* and the associated ρ_{eff} for various N_s/N using the parameters $N = 20$, $\mathcal{E} = 10$, $\mathcal{R}_g = 1$, and $\epsilon = 0$. The result in Proposition 3 correctly identifies all the optimum power allocation factors. Fig. 5 depicts the effective power ρ_{eff} as N_s increases with a fixed burst size N using either optimum power allocation β^* or fixed $\beta = 0.5$ and $\beta = 0.98$. The corresponding bit error rate (BER) performance versus N_s is depicted in Fig. 6. It is observed that the optimum β^* offers the best overall performance. When a fixed β is used, a larger N_s favors a larger β, and vice versa.

Lastly, for the equal per-symbol SNR case with $\mathcal{E}_{t,0} = \mathcal{E}_{s,0}$, we investigate the system-level impact of optimum number allocation. Fig. 7 depicts the achievable average capacity C for different numbers of allocation factors $N_s/N = \beta$. When a transmit reference transceiver [12] is used with $N_s = 0.5$ N, the average capacity is at most 0.5. Our optimum number allocation (labeled as "ES, optimum β^*") is able to asymptotically achieve capacity that is maximum even when unequal per-symbol SNR is allowed between training and information symbols. For different nominal SNR values ρ, the optimum number allocation versus the burst size is depicted Fig. 8. A larger burst size favors a larger percent of information symbols in order to maximize C.

VI. Conclusion

For ML optimum synchronizers with low symbol-rate sampling, a systematic design of transmission resource allocation

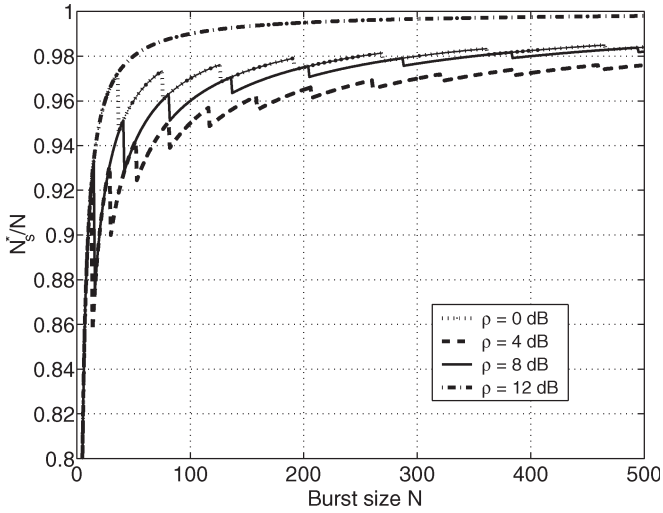

Fig. 8. Comparison of the optimum information number (data rate) N_s^*/N for various number allocation under the condition of equal per-symbol powers.

is provided in this paper, which jointly optimizes timing acquisition performance and information rate. The optimum transmission power and number allocation is analyzed not only for different subsets of the TS but also among the training and information-bearing symbols at the system level. Such results are useful in striking desirable performance-rate tradeoffs and achieving maximum system capacity under the total transmission resource constraints.

REFERENCES

[1] R. A. Scholtz, "Multiple access with time-hopping impulse radio," in *Proc. IEEE Military Communications Conf. (MILCOM)*, Boston, MA, Oct. 1993, pp. 447–450.

[2] M. Z. Win and R. A. Scholtz, "On the energy capture of ultrawide bandwidth signals in dense multipath environments," *IEEE Commun. Lett.*, vol. 2, no. 9, pp. 245–247, Sep. 1998.

[3] C. J. Le Martret and G. B. Giannakis, "All-digital impulse radio for wireless cellular systems," *IEEE Trans. Commun.*, vol. 50, no. 9, pp. 1440–1450, Sep. 2002.

[4] W. M. Lovelace and J. K. Townsend, "The effects of timing jitter and tracking on the performance of impulse radio," *IEEE J. Sel. Areas Commun.*, vol. 20, no. 9, pp. 1646–1651, Dec. 2002.

[5] E. A. Homier and R. A. Scholtz, "Rapid acquisition of ultra-wideband signals in the dense multipath channel," in *IEEE Conf. UWB Systems Technologies*, Baltimore, MD, May 2002, pp. 245–250.

[6] I. Maravic, M. Vetterli, and K. Ramchandran, "High-resolution acquisition methods for wideband communication systems," in *Proc. Int. Conf. Acoustics, Speech and Signal Processing (ICASSP)*, Hong Kong, Apr. 2003, pp. 133–136.

[7] Z. Tian and G. B. Giannakis, "BER sensitivity to mistiming in ultra-wideband impulse radios—Part I: Nonrandom channels," *IEEE Trans. Signal Process.*, vol. 53, no. 4, pp. 1550–1560, Apr. 2005.

[8] J. Foerster, "The effects of multipath interference on the performance of UWB systems in an indoor wireless channel," in *Proc. Veh. Technology Conf.*, Rhodes, Greece, 2001, pp. 1176–1180.

[9] V. Lottici, A. D'Andrea, and U. Mengali, "Channel estimation for ultra-wideband communications," *IEEE J. Sel. Areas Commun.*, vol. 20, no. 12, pp. 1638–1645, Dec. 2002.

[10] Z. Tian and G. B. Giannakis, "A GLRT approach to data-aided timing acquisition in UWB radios—Part I: Algorithms," *IEEE Trans. Wireless Commun.*, vol. 4, no. 6, pp. 2956–2967, Nov. 2005.

[11] A. R. Forouzan, M. Nasiri-Kenari, and J. A. Salehi, "Performance analysis of ultra-wideband time-hopping spread spectrum multiple-access systems: Uncoded and coded systems," *IEEE Trans. on Wireless Commun.*, vol. 1, no. 4, pp. 671–681, Oct. 2002.

[12] R. Hoctor and H. Tomlinson, "Delay-hopped transmitted-reference RF communications," in *IEEE Conf. UWB Systems Technologies*, Baltimore, MD, May 2002, pp. 265–269.

[13] H. Zhang and D. Goeckel, "Generalized transmitted-reference UWB communications," in *IEEE Conf. on UWB Systems Technologies*, Reston, VA, Nov. 2003, pp. 147–151.

[14] L. Yang and G. B. Giannakis, "Optimal pilot waveform assisted modulation for ultra-wideband communications," *IEEE Trans. Wireless Commun.*, vol. 3, no. 4, pp. 1236–1249, Jul. 2004.

[15] A. A. M. Saleh and R. A. Valenzuela, "A statistical model for indoor multipath propagation," *IEEE J. Sel. Areas Commun.*, vol. JSAC-5, no. 2, pp. 128–137, Feb. 1987.

[16] H. Lee, B. Han, Y. Shin, and S. Im, "Multipath characteristics of impulse radio channels," in *Proc. Veh. Technology Conf.*, Tokyo, Japan, Spring 2000, pp. 2487–2491.

Zhi Tian (S'98–M'00) received the B.E. degree in electrical engineering (automation) from the University of Science and Technology of China, Hefei, China, in 1994, and the M.S. and Ph.D. degrees from George Mason University, Fairfax, VA, in 1998 and 2000, respectively.

From 1995 to 2000, she was a Graduate Research Assistant at the Center of Excellence in Command, Control, Communications and Intelligence (C3I), George Mason University. Since August 2000, she has been with the Department of Electrical and Computer Engineering, Michigan Technological University, Houghton, where she is now an Associate Professor. Her current research focuses on signal processing for wireless communications, particularly on UWB systems.

Dr. Tian serves as the Associate Editor for the IEEE TRANSACTIONS ON WIRELESS COMMUNICATIONS. She was the recipient of a 2003 National Science Foundation (NSF) CAREER award.

Georgios B. Giannakis (S'84–M'86–SM'91–F'97) received the Diploma in electrical engineering from the National Technical University of Athens, Athens, Greece, in 1981, the M.Sc. degree in electrical engineering, the M.Sc. degree in mathematics, and the Ph.D. degree in electrical engineering from the University of Southern California (USC), Los Angeles, in 1983, 1986, and 1986, respectively.

After lecturing for one year at USC, he joined the University of Virginia, Charlottesville, in 1987, where he became a Professor of Electrical Engineering in 1997. Since 1999, he has been a Professor at the Department of Electrical and Computer Engineering, University of Minnesota, Minneapolis, where he now holds an ADC Chair in Wireless Telecommunications. His general interests span the areas of communications and signal processing, estimation and detection theory, time-series analysis, and system identification—subjects on which he has published more than 220 journal papers, 380 conference papers, and two edited books. Current research focuses on transmitter and receiver diversity techniques for single- and multiuser fading communication channels, complex-field and space-time coding, multicarrier UWB wireless communication systems, cross-layer designs, and sensor networks.

Dr. Giannakis was the corecipient of six paper awards from the IEEE Signal Processing (SP) and Communications Societies (1992, 1998, 2000, 2001, 2003, and 2004). He also received the IEEE-Signal Processing Society's Technical Achievement Award in 2000 and the European Association for Signal, Speech and Image Processing (EURASIP) Technical Achievement Award in 2005. He served as Editor-in-Chief for the IEEE SIGNAL PROCESSING LETTERS, as Associate Editor for the IEEE TRANSACTIONS ON SIGNAL PROCESSING and the IEEE SIGNAL PROCESSING LETTERS, as Secretary of the Signal Processing Conference Board, as Member of the Signal Processing Publications Board, as Member and Vice-Chair of the Statistical Signal and Array Processing Technical Committee, as Chair of the Signal Processing for Communications Technical Committee, and as a Member of the IEEE Fellows Election Committee. He has also served as a Member of the IEEE Signal Processing Society's Board of Governors, the Editorial Board for the PROCEEDINGS OF THE IEEE, and the Steering Committee of the IEEE TRANSACTIONS ON WIRELESS COMMUNICATIONS.